

COMPOSITIONAL CONSTRAINTS ON LUNAR SPINEL ANORTHOSITE: SYNTHESIS OF SPINEL WITH VARIABLE IRON CONTENT. C. R. M. Jackson¹, L. C. Cheek¹, S. W. Parman¹, R. F. Cooper¹, and C. M. Pieters¹
¹Dept. of Geological Sciences, Brown University, Providence, RI, 02912.

Introduction: Recent observations by the Moon Mineralogy Mapper (M^3) have identified spinel anorthosite within the lunar highlands [1,2]. Spinel anorthosite was not returned during the Apollo or Luna missions, leaving the petrogenesis of this lithology understudied and unclear [1]. Although similar to returned spinel troctolites [e.g. 3], the remotely sensed spinel anorthosites appear to have distinctly higher Mg/Fe, suggesting a unique, but perhaps related, petrogenetic history. Since identification, several spinel anorthosite formation hypotheses have been advanced, including assimilation of anorthosite by picritic liquid and melt-rock reaction of anorthosite and a Mg-suite parental liquid [4,5].

In this study, iron-bearing spinels were synthesized under reducing conditions applicable to the Moon. Reflectance spectra of these minerals were acquired in order to relate spectral features to measured compositional parameters. Spectral absorption position and strength are affected by the concentration of iron and other transition metals in spinel [6, 7], but these dependences are not well calibrated for the appropriate conditions (i.e. low Fe, low Cr, $\sim 10^{-1}$ fO_2). In particular, we aim to determine the amount of FeO necessary to generate a 1 μm absorption in spinel. This would allow constraints to be placed on the FeO content in the lunar spinel observed remotely, which have spectra lacking a 1 μm absorption.

Methods: Synthesis and Spectral Analysis: Reagent grade powders of MgO and Fe₂O₃ were ground and homogenized under ethanol using a mortar and pestle. Compacts of homogenized MgO-Fe₂O₃ powders and polyvinyl alcohol binder were cold-pressed at 100 MPa pressure and then placed on plates of high-purity (0.998+) Al₂O₃ (Figure 1). The compacts were 10 mm in diameter and 3 mm in height. The plate-compact pairs were placed on a bed of zirconia beads contained by an alumina boat. These boats were loaded into a gas mixing furnace and held at 1415°C and 1 atm for 65 hours. Streaming CO and CO₂ buffered the fugacity of oxygen to IW and reduced the Fe³⁺. At temperature, spinel was readily synthesized on the alumina plate where the compact was in direct contact, generating $\sim 200 \mu\text{m}$ thick spinel layers that are amenable to spectral analysis. The alumina plates bowed during synthesis, causing direct contact between the compact and plate to occur only within a central region. These central regions are circular and $\sim 5 \text{ mm}$ in diameter (Figure 1). The iron content of the spinel was controlled by varying the MgO/Fe₂O₃ of used to form the compact.

Spectra of the central regions for each run product were acquired in RELAB [8] using a Nicolet FTIR spectrometer. The data were collected as diffuse reflectance in both the near-IR (0.8-5 μm) and mid-IR (5-25 μm) wavelength ranges.

Results: Morphology & Major Elements: The alumina plates were sectioned normal to the spinel growth face. The exposed faces were then mounted and analyzed by electron microprobe (EMPA, MIT, JEOL JXA-8200) for major element composition. Importantly, transects across the central regions revealed only minor compositional variability (Figure 2). Compositional homogeneity indicates the spectra from the central regions are representative of specific Fe-bearing spinel compositions. Major elements of the reported spinel are given in Table 1.

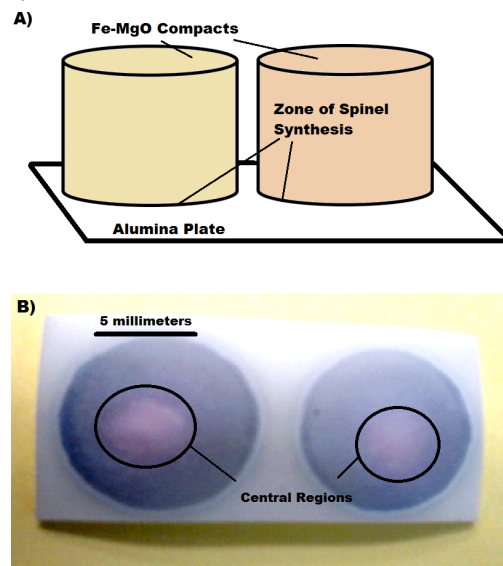


Figure 1: A) Diagram of experimental setup and B) picture of representative run products. Compacts with different Fe/Mg (represented by different color in 1a) were placed on alumina plates. The central regions are the areas where the compacts remained in direct contact with the plate for the duration of the experiment. These are the regions where the reported spinel spectra were taken.

Lower-Fe-content central regions and all analyzed circum-central regions contained elevated Ni concentrations (>0.15 and $<1.6 \text{ wt } \%$). The spectra of areas with high Ni concentrations (indicated by blue color and compositional analysis) contained prominent 1 μm absorptions, despite low FeO concentrations (0.2 wt %). Consequently, we only use the spectra from central regions with low Ni concentrations ($<0.075 \text{ wt } \%$) to constrain the lunar crust spinel composition of the newly identified spinel anorthosite. We believe Ni was intro-

duced into the system via vapor phase transport, sourced from the refractory boats that had been exposed to NiO in previous experiments.

	Al ₂ O ₃	FeO	MgO	NiO	Cr ₂ O ₃	MnO	TiO ₂	Total
Spinel 1	71.78	5.13	22.78	0.01	0.00	0.02	0.00	99.73
std dev	1.06	0.24	1.27	0.01	0.00	0.02	0.00	
Spinel 2	73.05	4.85	22.76	0.06	0.00	0.00	0.01	100.73
std dev	1.89	0.42	2.31	0.01	0.00	0.00	0.01	
Spinel 3	72.63	2.82	24.57	0.04	0.02	0.04	0.00	100.12
std dev	0.64	0.27	1.17	0.01	0.01	0.01	0.00	

Table 1: Average of points analyzed (EMPA) for central regions of spinel and associated standard deviations on the average. FeO standard deviations are small, indicating differences in the IR spectra of the spinel represent significant precision.

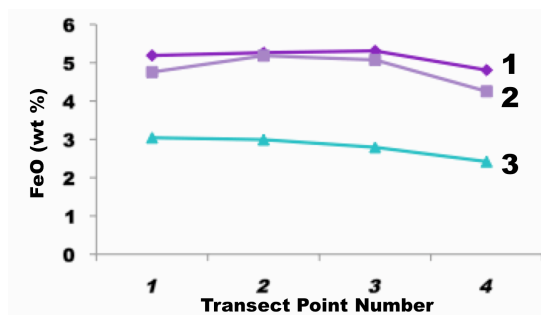


Figure 2: Results of EMPA transects across exposed face of central regions. Transects were diagonal, extending from the base of the spinel layer (Point 1), to the surface (Point 4), at an angle. Transects contained evenly spaced points and were ~200 μm in length. The synthesized spinels have a narrow compositional range for given compact-plate pairing.

Results: Spectral Properties: Spectra of all samples show a broad absorption in the 2-3 μm region (Fig. 3a), consistent with documented spectral properties of natural spinel [5, 6]. This prominent feature likely represents two overlapping absorptions at ~2.0 and ~2.8 μm , each due to electronic transitions in Fe²⁺ in a tetrahedral site. These strong absorptions are apparently saturated even at ~3 wt% FeO. Mid-IR spectra of the same samples are also consistent with Mg-spinel compositions (Fig. 3b).

1 μm absorption: Spinel 3, with only ~3% FeO, does not show a strong 1 μm band, while Spinel 1 and 2 (~5% FeO), do have a notable feature in this range. This is consistent with other work suggesting that a 1 μm band occurs in spinels due to Fe²⁺ in octahedral coordination [5, 6] and preliminarily supports that at least ~5 wt.% FeO is required.

Conclusions: Synthesis experiments under lunar-like reducing conditions have produced homogeneous, Mg-rich spinels with variable FeO content. Near-IR reflectance spectra of synthetic spinels with $\geq 5\%$ FeO show a 1 μm absorption, while the one sample with $< 5\%$ FeO does not. We stress that these are preliminary results, but they suggest that the Mg-spinels detected by M³ on the lunar surface, which do not show a 1 μm feature, have

very low FeO contents ($< \sim 5\%$). Such a low FeO content would require a high Mg# liquid in the petrogenesis of these spinels. The aluminate spinel-olivine $K_d^{\text{Fe}^{2+}\text{-Mg}}$ is close to one [9], indicating the liquid reacting to produce the spinel anorthosite would be in equilibrium with a $> \text{Fo}90$ olivine. This is too Mg-rich for the most magnesian picrites [10] and points towards the involvement of Mg-Suite liquids. Incorporation of small amounts of Cr into the spinel would increase the Fo content of the equilibrium olivine [10]. Future work will focus on producing additional synthetic spinels with finer variations in FeO in order to better constrain the onset of a 1 μm absorption.

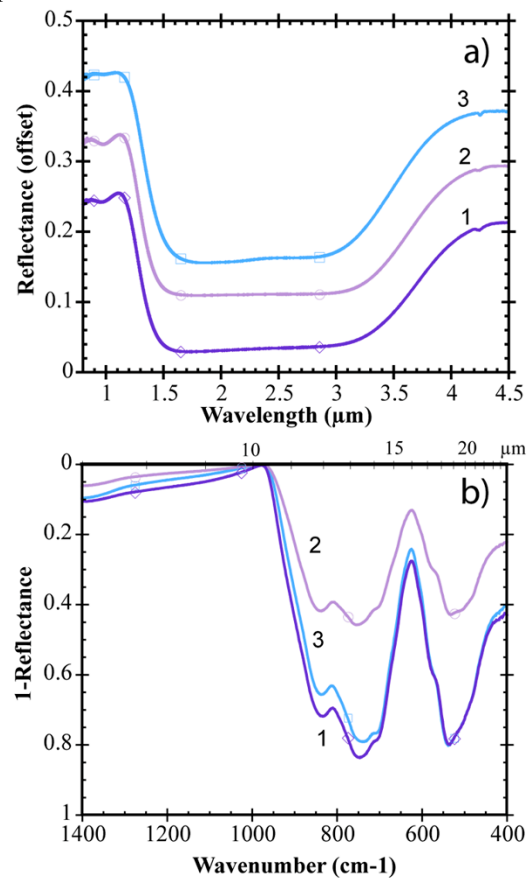


Figure 3: Reflectance spectra of Spinel 1, 2, and 3 in a) NIR and b) MIR wavelengths. A prominent 2-3 μm absorption is present in all run products, but the 1 μm band is only present in the spinels with FeO $\geq 5\%$.

Acknowledgements: RELAB is a multiuser facility supported by NASA grant NNG06GJ31G. CRMJ and LCC benefitted from the Spring-Fall 2011 lunar seminar held at Brown in developing this collaboration.

References: [1] Pieters C.M. et al. (2011), *JGR*, 116, E00G08 [2] Dhingra, D et al. (2011), *GRL*, 38, L11201 [3] Haggerty S.E. (1973) *Geochim. Cosmo. Acta*, 37, 857-867 [4] Gross J. & Treiman A.H. (2011), 116, E10009 [5] Ganskow G. et al. (2011) EOS trans. P13D-1695 [6] Burns R. G. (1993) *Mineralogical Applications of Crystal Field Theory* Cambridge University Press, 551. [7] Cloutis E.A., (2004) *MAPS*, 39, 545-556. [8] Pieters C. M. (1983) *JGR*, 88, 9534-9544 [9] Jamieson and Roeder, (1984), *Am. Min.*, 69, 283-291 [10] Elkins-Tanton L.T. et al. (2003) *MAPS*, 38, 515-527